Article

Study on the Variations of Key Groups and Thermal Characteristic Parameters during Coal Secondary Spontaneous Combustion

Jiangbo Guo, Tianjun Zhang,* and Hongyu Pan

Read Online

ACCESS | Metrics & More | Article Recommendations

ABSTRACT: To investigate the effect of preoxidation on the secondary spontaneous combustion of coal, the changes in the key groups and thermal characteristic parameters in coal after preoxidation were investigated through Fourier transform infrared spectroscopy (FTIR), laser thermal conductivity, and thermogravimetric experiments. Results showed that the aromatic hydrocarbons in coal gradually decrease with the rise in the preoxidation temperature, the aliphatic hydrocarbons increase and then decrease, the −C−O− group gradually decreases, and the −C═O and −COO− group content slowly increases. Preoxidation promotes the breakdown of aromatic hydrocarbons and the oxidation of oxygen-containing functional groups in coal. Meanwhile, the thermal diffusivity of coal decreases after preoxidation, while the specific heat capacity and thermal conductivity increase and then decrease. The results of the thermogravimetric analysis indicate that preoxidation changes the characteristic temperature, but it does not change the process of spontaneous combustion. The spontaneous combustion process of raw and preoxidized coals can be divided into three stages: water evaporation, oxygen adsorption, and combustion. Further, the apparent activation energy increases and then decreases with a rise in the preoxidation temperature during the moisture evaporation stage, increases during the oxygen adsorption stage, and decreases during the combustion stage.
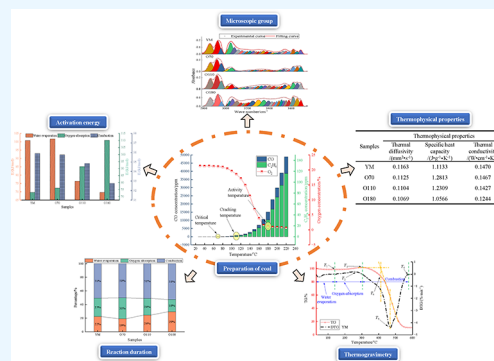
1. INTRODUCTION

Coal occupies an important position in the world's energy mix as an essential energy product and industrial raw material.[1−3] Global coal production exceeds 8.1 billion tonnes,[4] accounting for roughly 27% of the primary energy applications.[5] However, coal spontaneous combustion disasters are also widespread in major coal-producing regions, such as China, the USA, and Australia, causing serious economic losses and environmental hazards.[6−9] Many fire areas are subject to reignition after the coal fires have been extinguished due to the complexity of the mining conditions and the specific nature of coal.[10,11] The material composition and microstructure of these coals, which have undergone primary oxidation, are more profoundly altered, resulting in a secondary spontaneous combustion process that differs from the primary spontaneous combustion of coal.[12−14] Therefore, an in-depth study of the secondary spontaneous combustion of coal must be conducted.

Coal spontaneous combustion is caused by the potent exothermic reaction of microscopic groups in coal with oxygen. Accordingly, it is significant to understand the variation of coal microscopic groups to explore the secondary spontaneous combustion process of coal. Xiao et al.[15] studied the changes and reaction processes of each major functional group during the secondary oxidation of coal. Liang et al.[16] investigated the effects of preoxidation on the reactive functional groups and pore morphology of coal through FTIR and SEM experiments.

The result showed that the secondary oxidation of coal was promoted with the increase in reactive groups and pore size in coal after preoxidation. Zhao et al.[17] demonstrated that the oxygen-containing functional groups formed by preoxidation of quasi-east coals significantly enhanced the gasification reaction activity of coke, resulting in a 32% reduction in the activation energy of the gasification reaction. Jo et al.[18] concluded that the aliphatic hydrocarbon and ether bond content of coals significantly decreased after preoxidation. Xu et al.[19] investigated the effect of water leaching and preoxidation on the microscopic groups of coal and found that the contents of the −OH, −C═O, and −COOH groups significantly increased in coals that were preoxidized and water leached. Xu et al.[20] suggested that preoxidation could enhance the oxidation of the aliphatic hydrocarbon structures and promote their secondary oxidation process.

With regard to the study on the effect of preoxidation on the macroscopic parameters of coal, Álvarez et al.[21] proposed that
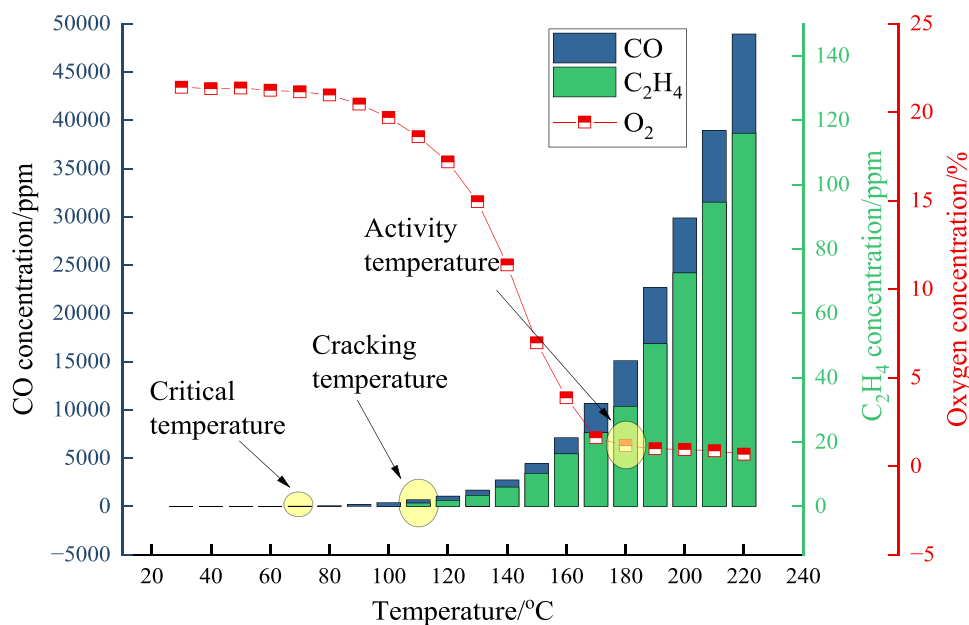
Figure 1. Variation of indicator gases during low-temperature oxidation of coal.

the gasification reactivity of coal will be improved after preoxidation at 200−300 °C in the air atmosphere. Pis et al.[22] investigated the effect of preoxidation on the early autothermal behavior of coal using differential thermal analysis. Wang et al.[23−25] concluded that the characteristic parameters, such as exotherm, gas products, and the apparent activation energy of coal, more significantly changed after preoxidation. Tang et al.[26] studied the mass and heat changes after preoxidation and concluded that preoxidation increases the risk of spontaneous combustion of lignite, but excessive preoxidation temperatures have the opposite effect. Deng et al.[27] showed that the CO concentration, oxygen consumption rate, and exothermic rate during the secondary oxidation of preoxidized coals were significantly higher than those of the original coal. Lü et al.[28] considered that the exothermic temperature of coal undergoing preoxidation treatment would be lagged and the heat release and maximum heat release power would be less than that of the original coal. Zhang et al.[29] suggested that nitrogen had a significant inhibitory effect on the secondary oxidation process of coal.

In conclusion, sufficient research has been carried out at this stage on the secondary oxidation of coal. However, a comprehensive study on the microscopic groups and heat transfer capacity and thermal behaviors of preoxidized coals is not available. In this work, FTIR and laser thermal conductivity experiments were conducted to investigate the changes in the microscopic groups and thermal physical parameters of raw and preoxidized coals. Thermogravimetric experiments were also employed to investigate the variations in the thermal and kinetic parameters during the spontaneous combustion of raw and preoxidized coals and clarify the effect of initial oxidation on the secondary spontaneous combustion of coal. The results of this work contribute to the investigation of the mechanism of reignition of legacy coal and the prevention and control technology of coal spontaneous combustion hazards.

2. SAMPLES AND EXPERIMENTS

2.1. Preparation of Samples. Bituminous coal from Shandong Province, China, was utilized for the investigation. The unoxidized coal cores were collected, ground, and crushed. A vibrating screen is used to screen the coal samples with different crushing degrees, and coal samples with particle sizes between 0.1 and 0.15 mm are selected for the experiment. A temperature-programmed device was used to oxidize raw coal and details of the device can be found in a previous study.[30,31] The mass of the coal sample was 100 g, the heating rate was 1 °C/min, the flow rate of the experimental gas was 50 mL/min, and the gas composition was dry air, that is, the volume fraction of oxygen was 21%. The gas produced by oxidation in the coal sample tank was extracted at 10 °C intervals and the composition and content of the gas were analyzed through gas chromatography. In the actual production of the mine, the changes in the CO and C_2H_4 gases are commonly used to determine the degree of development of the spontaneous combustion of coal. Meanwhile, oxygen is necessary for the spontaneous combustion of coal. Accordingly, the CO, C_2H_4, and oxygen concentrations were selected as indicator gases for the determination of the spontaneous combustion process. The changes in indicator gases during the heating of coal spontaneous combustion are shown in Figure 1. A more pronounced shift or change in the indicator gases of coal can be observed at 70, 110, and 180 °C. CO from low-temperature coal oxidation begins to significantly increase at 70 °C, C_2H_4 gas appears at 110 °C, and the oxygen concentration begins to turn at 180 °C. In particular, 70, 110, and 180 °C are the critical, cracking, and activity temperatures of coal during spontaneous combustion, respectively. Different characteristic temperatures mean that coal enters into various reaction processes and this is also the most common indicator of the process of coal spontaneous combustion in practical coal mines. Accordingly, these three temperatures were chosen for the preparation of preoxidized coals and named O70, O110, and O180. Unoxidized coal was named YM. The proximate analysis data of the raw coal and preoxidized coal samples are shown in Table 1. The results showed that the volatile content

Table 1. Proximate Analysis Data of Coal Samples

sample	proximate analysis			
	M_{ad}, %	A_{ad}, %	V_{ad}, %	FC_{ad}, %
YM	1.48	11.23	31.55	55.74
O70	1.38	11.31	31.85	55.46
O110	1.76	11.46	29.61	57.17
O180	1.21	11.36	28.01	59.42

of coal gradually decreases with the increase in the oxidation temperature, while the fixed carbon content slowly increases. This finding implies that coal's composition is altered during preoxidation, which may alter coal's spontaneous combustion.

2.2. Experimental Apparatus. *2.2.1. Fourier Transform Infrared Spectroscopy (FTIR) Experiments.* Fourier transform infrared spectroscopy (Nicolet iN10 and iZ10, Thermo Fisher) was used to test the microscopic group changes of raw and preoxidized coal. The tests were carried out using the potassium bromide pressure method, with the instrument set to 32 scans, a wave number range of 600−4000 cm^{-1}, and a resolution of 4 cm^{-1}. To reduce the error in curve comparison, the mass ratio of potassium bromide to the coal sample in each test is 150:1 and the mass of the coal sample is 1 mg.

2.2.2. Laser Thermal Conductivity Experiments. A laser thermal conductivity meter (LAF457, NETZSCH, Germany) was employed to test the variation of the thermophysical properties of raw and preoxidized coals. The principle of the test is the laser flash method, whereby a thin circular coal sheet with a homogeneous texture is irradiated with a laser to test the temperature variation over time and is compared with a ceramic sheet with known thermophysical properties to determine the three key thermophysical properties of coal: thermal diffusivity, specific heat capacity, and thermal conductivity. The thin round coal flakes were formed by pressing at 30 MPa for 5 min using a hydraulic press.

2.2.3. Thermogravimetric Experiments. Thermogravimetric analysis (449F3, NETZSCH, Germany) was carried out on raw coal and preoxidized coal to test for mass changes during spontaneous combustion. A single test was carried out with a 5 mg mass of the coal sample, a temperature range of 30−600 °C, and a rate of 5 °C/min. A gas mixture with a flow rate of 50 mL/min and a nitrogen-to-oxygen volume ratio of 79:21 was used to maintain the reaction.

3. RESULTS AND DISCUSSIONS

3.1. Variation of Microscopic Groups in Coal Samples. The exothermic reaction of the microscopic groups with oxygen is the essence of the spontaneous combustion of coal and is one of the main causes of spontaneous combustion disasters. Coal is a complex mixture of macromolecules and contains many different microscopic groups, such as −OH, −CH$_3$, and −C≡C−. The mixture of these micro-groups determines the reactivity of different coals and, to some extent, the course of spontaneous combustion development. Accordingly, the FTIR data of raw coal and preoxidized coals were tested to more accurately measure the variation of the spontaneous combustion of coal after preoxidation, as shown in Figure 2. The results suggested that significant differences exist between preoxidized coal and raw coal. For example, a clear difference exists between the FTIR curves of raw and preoxidized coals at wave numbers of 3200−3600 cm^{-1}, and these ranges are dominated by the various types of hydroxyl groups and free and associated hydrogen bonds. At wave numbers around 1750 cm^{-1}, that is, the absorption peak of the −COO− group, O180 shows a clear absorption peak, while the FTIR peaks of the rest of the coal samples are flat. The absorption peak of Ar−CH in YM is significantly stronger than that of the other coal samples at a wave number of 3050 cm^{-1}. The variation in FTIR curves implies that the microscopic groups of coal have significantly changed after oxidation. The FTIR data were fitted to the peaks using the Fourier deconvolution method to accurately measure the microscopic group changes in each coal sample. The results are shown in Figure 3. The microscopic groups of coal were classified into three main groups, namely, oxygenated functional groups, aliphatic compounds, and aromatic compounds, based on the position of the attributed infrared absorption peaks in coal.[32−34] According to the Lambert−Beer law, the content of functional groups is proportional to their corresponding peak areas in the spectrum. The contents of the different microscopic groups of raw and preoxidized coals were determined and compared based on the area of the fitted peaks. The oxygen-containing functional groups include −OH, −C−O−, −C≡O, and −COO− and the aliphatic compounds include −CH$_3$, −CH$_2$−, and aliphatic−CH(Al−CH), while the aromatic compounds include −C≡C−, aromatic−CH-(Ar−CH), and substituted benzene.
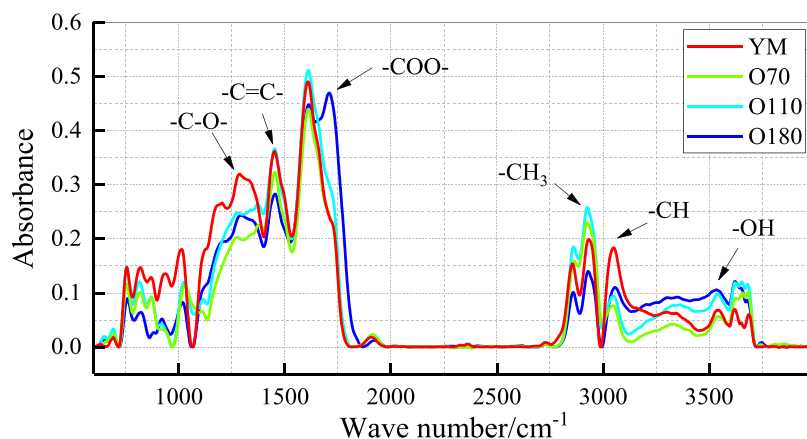

Figure 2. Comparison of the FTIR curves of raw coal and preoxidized coals.
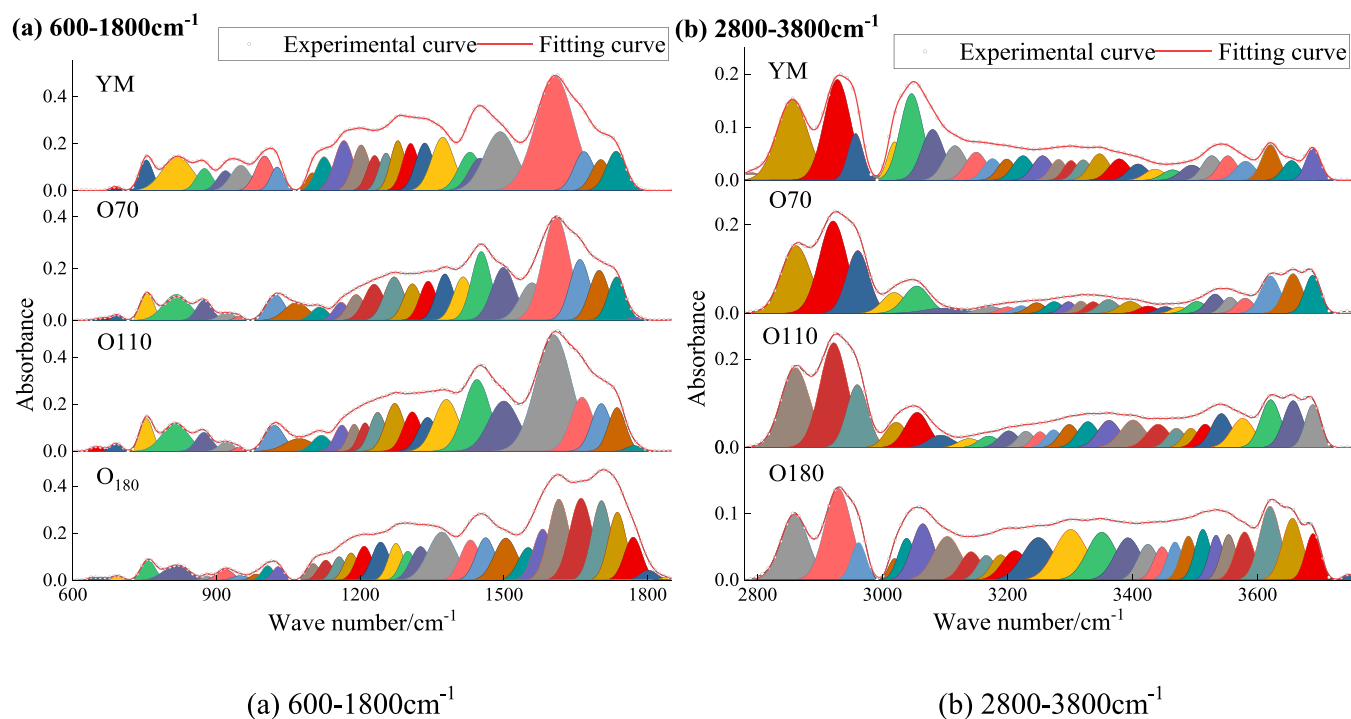
(a) 600-1800cm⁻¹

(b) 2800-3800cm⁻¹

Figure 3. FTIR fitting process of raw coal and preoxidized coals.
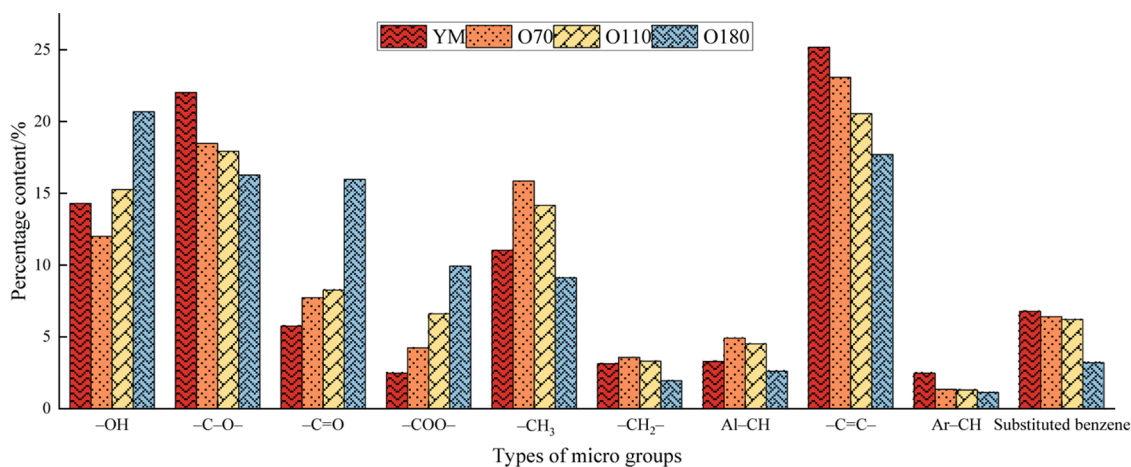

Figure 4. Variations of key microgroups content of raw coal and oxidized coals.

Figure 4 illustrates the variation in the content of the 10 key groups in raw and preoxidized coals. Preoxidation has a relatively obvious effect on the content of the key groups in coal. The content of the three aromatic hydrocarbon compounds in coal significantly decreased after preoxidation. The degree of decrease was proportional to the preoxidation temperature. The aromatic hydrocarbon compounds, especially the −C═C− group, are considered to be the core of the coal macromolecular structure. The decrease in the content of aromatic hydrocarbon compounds implies that preoxidation leads to the cleavage of the molecular core of coal, which is centered on the aromatic ring. The higher the preoxidation temperature, the stronger the cleavage. The contents of −CH₃, −CH₂, and Al−CH, the three aliphatic hydrocarbon groups, increase and then decrease with increasing preoxidation temperature. For example, the −CH₃ content of YM is 11.0%, while the CH₃ contents of O70, O110, and O180 are 15.9, 14.1, and 9.1%, respectively. Aliphatic hydrocarbon

compounds are the key linking groups in coal and are formed as bridge bonds between macromolecules and as side chains. The results in Figure 4 showed that preoxidation at lower temperatures increases the number of side chains in coal, with this increase in side-chain aliphatic hydrocarbons coming partly from the breaking of long-chain aliphatic and bridging bonds and partly from the cleavage of aromatic hydrocarbons. When the preoxidation temperature is further increased, the rate of production of the aliphatic side chains in coal is lower than the rate of consumption, resulting in a reduction in the content of aliphatic compounds in the O180 coal sample. The oxygen-containing functional groups are considered to be one of the most important groups in the spontaneous combustion process of coal and their reaction with oxygen is one of the significant causes of the spontaneous combustion of coal.[35,36] The four oxygen-containing functional groups showed different trends as the preoxidation temperature increased, with the −OH group first decreasing and then increasing, the −C−O−

group gradually decreasing, and the −C═O and −COO− group contents slowly increasing. Relating this change to the trend in the content of aliphatic compounds, preoxidation promotes the conversion of aliphatic compounds in coal to −OH. In addition, the changes in the content of the remaining three oxygen-containing functional groups imply that preoxidation leads to the oxidation of the more primary oxygen-containing functional groups in coal, such as −C−O−, to the double bonded −C═O and −COO− groups.

3.2. Variation in the Thermophysical Properties of Coal Samples.
Thermal diffusivity, specific heat capacity, and thermal conductivity are the three thermophysical properties that describe a substance's heat transfer capacity. Their definitions and calculation methods can be found in the previous literature.[37,38] Table 2 displays the three thermophys-

Table 2. Variation of Thermophysical Properties of Raw Coal and Preoxidized Coals

samples	thermophysical properties		
	thermal diffusivity $(mm^2 \cdot s^{-1})$	specific heat capacity $(J \cdot g^{-1} \cdot K^{-1})$	thermal conductivity $(W \cdot cm^{-1} \cdot K^{-1})$
YM	0.1163	1.1133	0.1470
O70	0.1125	1.2813	0.1467
O110	0.1104	1.2309	0.1427
O180	0.1069	1.0566	0.1244

ical properties of raw and preoxidized coals obtained from the laser thermal conductivity experiment. The primary oxidation temperature has a more pronounced effect on the thermophysical properties of the coal samples. The thermal diffusivity of preoxidized coal progressively decreases as the oxidation temperature rises compared with raw coal, while the specific heat capacity and thermal conductivity increase and eventually gradually decline. The specific heat capacity indicates the speed of temperature rise of a substance under the same conditions. The larger the specific heat capacity, the more the heat that is required for the temperature rise, that is, the worse the temperature rise effect. Thermal diffusivity and conductivity are physical quantities that measure the ability of a substance to conduct temperature and transfer heat, respectively, and higher thermal diffusivity and conductivity mean that the transfer of temperature and heat is more favorable during the spontaneous combustion of coal. The results in Table 2 indicate that the heat transfer and thermal conductivity of coal deteriorate after preoxidation. This condition probably occurs because preoxidation destroys the orderliness and stability of the structure of the coal itself, resulting in certain inhibition of temperature and heat transfer. The change in specific heat capacity indicates a more convenient increase in temperature during spontaneous combustion of the O180 coal sample under the same heat storage conditions. Meanwhile, the O70 coal sample has a weaker ability to raise temperature than the original coal. This phenomenon may lead to a more pronounced temperature rise difference between preoxidized coal and the original coal during secondary spontaneous combustion.

3.3. Variation in the Coal Mass During Secondary Spontaneous Combustion.
According to the research above, the preoxidation of coal causes major changes in its material composition, microgroups, and thermophysical properties, which unavoidably causes considerable changes in the spontaneous combustion process. Thermogravimetric tests

were conducted to test the mass variations of raw and preoxidized coals during the process to ascertain the impact of preoxidation on the secondary oxidative spontaneous combustion of coal. The results are displayed in Figure 5. The course of the spontaneous combustion reaction for raw and preoxidized coals can be divided into three stages: water evaporation, oxygen adsorption, and combustion. Overall, water in the coal sample begins to evaporate during the initial heating, resulting in a slight decrease in the coal mass. After the evaporation of free water from the sample, the pores in coal further increase and coal begins to slowly adsorb oxygen, resulting in a slow increase in mass. At a temperature of ∼300 °C, the mass of oxygen adsorbed by coal reaches its maximum and the aliphatic compounds in coal, mainly −CH$_3$ and −CH$_2$−, begin to decompose, resulting in a slow decrease in mass. The aromatic compounds in the coal sample begin to depolymerize with the further increase in the reaction temperature, generating a large number of reactive free radicals. Further oxidative combustion of these radicals with oxygen results in a rapid decrease in the mass of the coal sample. After the organic matter in coal has been burnt out, the quality of the sample plateaus. Six characteristic temperature points were identified to characterize the process of spontaneous combustion of coal based on the change in mass during the secondary spontaneous combustion of raw and preoxidized coals.[39] The results are shown in Table 3.

The results in Table 3 show that preoxidation has a more pronounced effect on the characteristic temperature during the secondary spontaneous combustion of coal and the variation in characteristic temperature is not identical from one to another. Overall, the differences in characteristic temperatures can be divided into two categories. The first category includes T_1, T_2, and T_3, which significantly differ from each other, while T_4, T_5, and T_6 fall into the second category with a slight difference. For example, the differences in T_1 and T_2 between O70 and YM are 17.6 and −7.5 °C, respectively. Meanwhile, the differences in T_4 and T_5 between the two are only −0.4 and 0.9 °C, respectively. This result implies that preoxidation has a greater effect on the early stages of coal spontaneous combustion and a minor effect on the later stages. Such a phenomenon occurs because the dominant reaction of coal spontaneous combustion is the combustion reaction of volatile fraction and fixed carbon with oxygen in coal after the temperature exceeds T_3 (i.e., after entering the combustion stage). Meanwhile, the total content of volatile fraction and fixed carbon of preoxidized coal slightly changes, and its influence on the combustion stage is smaller. By contrast, the reaction between coal and oxygen in the low-temperature oxidation stage is dominated by the oxidation of the various groups in the coal, particularly oxygen-containing functional groups, with significant variations in the microscopic group content of the different preoxidized coals, resulting in major differences in the preoxidation stage of coals.

Further observations reveal significant differences in the characteristic temperatures of the different temperature preoxidized coals. For example, O70 has a minimum T_1 and a maximum T_3, while O180 is exactly the opposite. The percentage of the time spent in different stages of secondary spontaneous combustion between raw and preoxidized coals was determined based on the key characteristic temperature nodes and stage divisions in Figure 5 and Table 3 to further determine the effect of preoxidation on the process of coal spontaneous combustion, as shown in Figure 6. The results
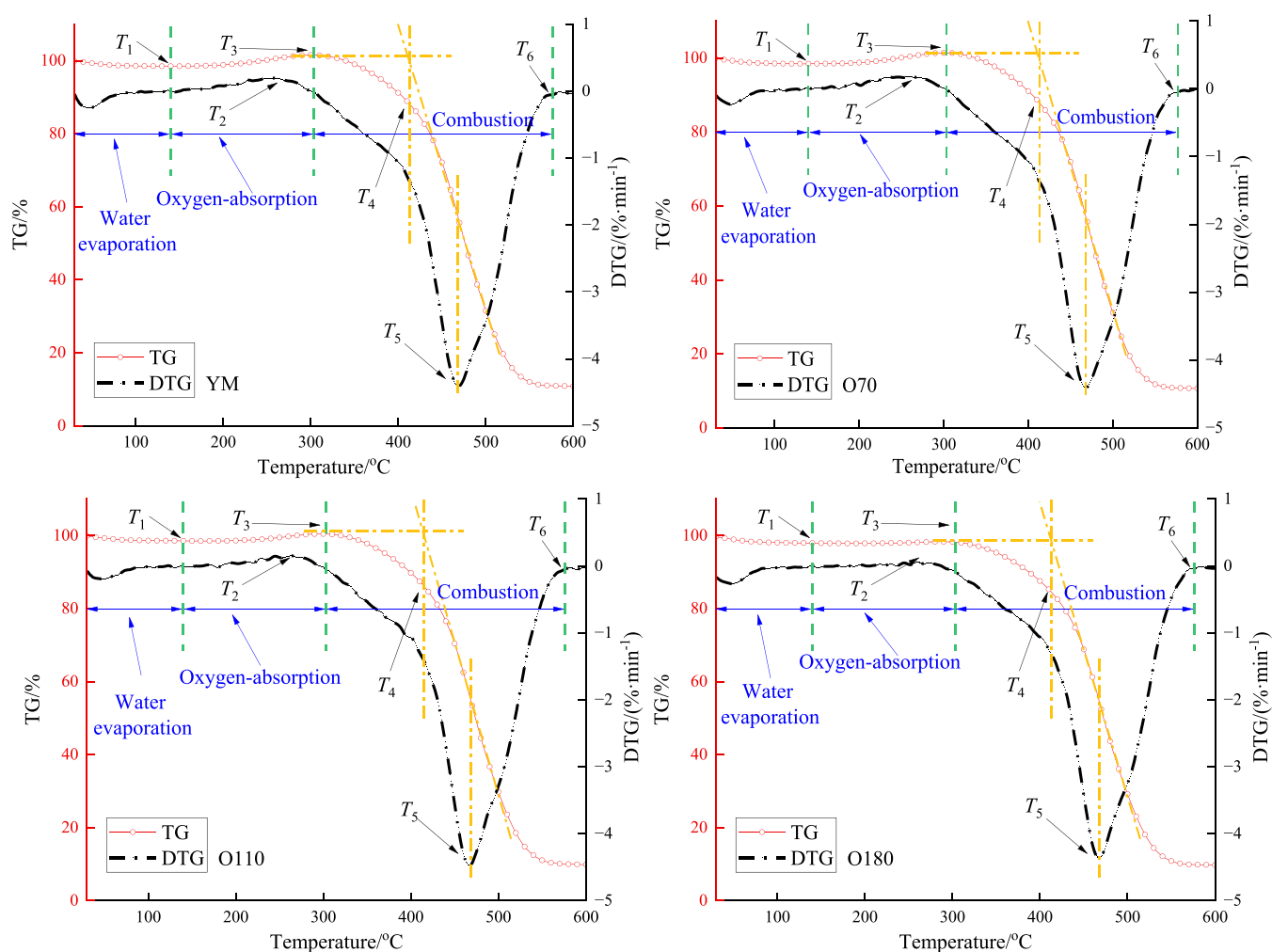
Figure 5. Mass change of coals during secondary spontaneous combustion.

Table 3. Characteristic Temperature of the Coal Sample During Secondary Spontaneous Combustion

samples	characteristic temperature, °C					
	T_1	T_2	T_3	T_4	T_5	T_6
YM	151.5	250.7	298.6	419.2	468.7	574.7
O70	133.9	258.2	301.1	419.6	467.8	575.1
O110	163.2	256.1	295.6	419.1	467.0	573.8
O180	189.9	255.5	287.3	419.0	465.8	573.1

showed that the duration of the three reaction stages varied for different coal, while the overall time of secondary spontaneous combustion remained basically the same. The duration of the water evaporation stage decreases and then increases with the rise in the preoxidation temperature. Meanwhile, the duration of the oxygen uptake and weight gain stage increases and then increases, while the combustion stage tends to decrease and then increase, but the change is small compared with the overall duration. This finding is consistent with the results of the analysis in Table 3, where preoxidation has a greater effect on the low-temperature oxidation stage and a smaller effect on the high-temperature combustion stage. Furthermore, O70 has the shortest water evaporation stage and the longest oxygen uptake weight gain stage, indicating that the O70 coal sample is more likely to reach T_1 during spontaneous combustion but needs to undergo a longer oxygen uptake weight gain stage to

completely burn. The opposite is true for the O180 sample. After a relatively long water evaporation stage, O180 undergoes a shorter oxygen uptake and weight gain stage, resulting in a minimum time for combustion to occur with oxygen. This finding remains consistent with the analytical results of the thermal properties in Table 2.

3.4. Variation in Kinetic Parameters of Secondary Coal Spontaneous Combustion Processes. The kinetic parameters reflect the reaction characteristics of coal and oxygen at different stages. According to the Arrhenius formula, the reaction rate between coal and oxygen has the following law:[40,41]

$$\frac{d\alpha}{dt} = A \exp\left(\frac{-E}{RT}\right) f(\alpha) \tag{1}$$

Variable α is the conversion rate of coal during spontaneous combustion; A is the pre-exponential factor; E is the apparent activation energy of the reaction, kJ/mol; R is the general constant of a standard gas, 8.314 kJ/(mol·K); and $f(\alpha)$ is the differential form of the mechanism function. The commonly used Achar method for computational kinetics is obtained by the logarithmic transformation of eq 1, as shown in eq 2.[42,43]

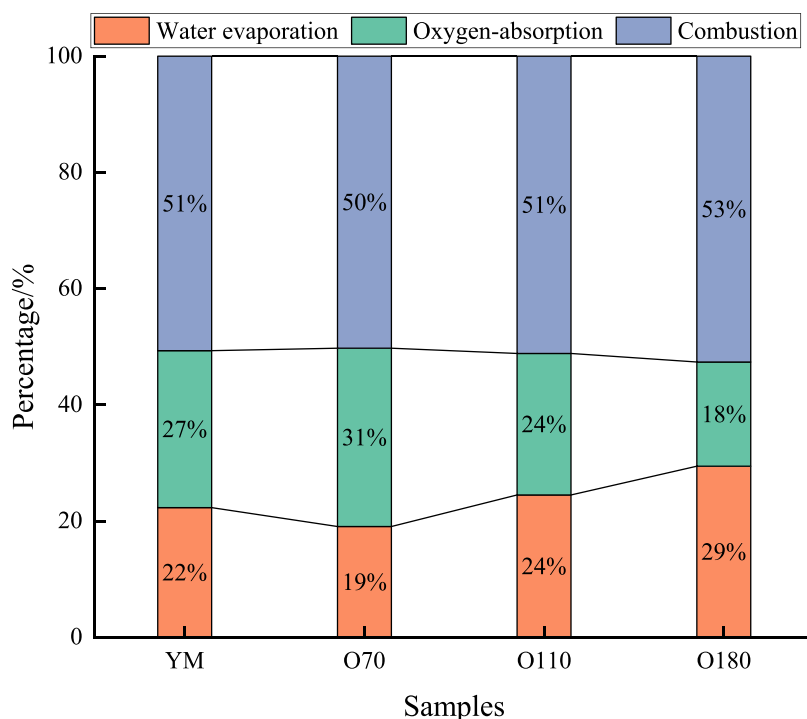$$\ln \frac{d\alpha/dt}{f(\alpha)} = \ln A - \frac{E}{RT} \tag{2}$$

Figure 6. Duration of different stages of coal secondary spontaneous combustion.

Table 4. Summary of Expressions for Mechanistic Functions

no.	reaction model	symbol	$f(\alpha)$	$G(\alpha)$
		Reaction Order		
1	zero-order	O0	1	α
2	first-order	O1	$1 - \alpha$	$-\ln(1 - \alpha)$
3	one and half order	O3/2	$(1 - \alpha)^{3/2}$	$2[(1 - \alpha)^{-1/2} - 1]$
4	second-order	O2	$(1 - \alpha)^2$	$(1 - \alpha)^{-1} - 1$
5	third-order	O3	$(1 - \alpha)^3$	$1/2[(1 - \alpha)^{-2} - 1]$
		Growth Models		
6	power law	P2/3	$2/3\alpha^{-1/2}$	$\alpha^{3/2}$
7	power law	P2	$2\alpha^{1/2}$	$\alpha^{1/2}$
8	power law	P3	$3\alpha^{2/3}$	$\alpha^{1/3}$
		Nucleation Models		
9	Avrami−Erofeev	A1	$3/2(1 - \alpha)[-\ln(1 - \alpha)]^{1/3}$	$[-\ln(1 - \alpha)]^{2/3}$
10	Avrami−Erofeev	A2	$2(1 - \alpha)[-\ln(1 - \alpha)]^{1/2}$	$[-\ln(1 - \alpha)]^{1/2}$
11	Avrami−Erofeev	A3	$3(1 - \alpha)[-\ln(1 - \alpha)]^{2/3}$	$[-\ln(1 - \alpha)]^{1/3}$
		Stage Boundary Controlled Reaction		
12	contracting cylinder	R2	$2(1 - \alpha)^{1/2}$	$1 - (1 - \alpha)^{1/2}$
13	contracting sphere	R3	$3(1 - \alpha)^{2/3}$	$1 - (1 - \alpha)^{1/3}$
		Diffusion		
14	one-dimensional diffusion	D1	$1/(2\alpha)$	α^2
15	two-dimensional diffusion	D2	$-[\ln(1 - \alpha)]^{-1}$	$(1 - \alpha)\ln(1 - \alpha) + \alpha$

According to the Achar method, $\ln\dfrac{d\alpha / dt}{f(\alpha)}$ and $1/T$ show an obvious linear relationship. Therefore, the mass data in the process of coal spontaneous combustion are calculated and brought into the equation. The slope and intercept of the straight line are obtained by fitting with the least square method. Then, the apparent activation energy and pre-exponential factor of the reaction are determined.

An integral transformation of eq 1 is performed and the heating rate is introduced to obtain the commonly used kinetic Coats−Redfern method, as shown in eq 4.[44,45] Variable β is the

heating rate (°C/min) and $G(\alpha)$ is the integral form of the mechanism function.

$$\ln\left[\frac{G(\alpha)}{T^2}\right] = \ln\left(\frac{AR}{\beta E}\right) - \frac{E(\alpha)}{RT} \tag{3}$$

The slope and intercept of the line fitted with $\ln\left[\dfrac{G(\alpha)}{T^2}\right]$ and $1/T$ in the Coats−Redfern method can determine the apparent activation energy and pre-exponential factor of the reaction. In eqs 2 and 3, the reaction conversion α is calculated, as shown in eq 4.[46] M_0 and M_e are the coal sample masses at the
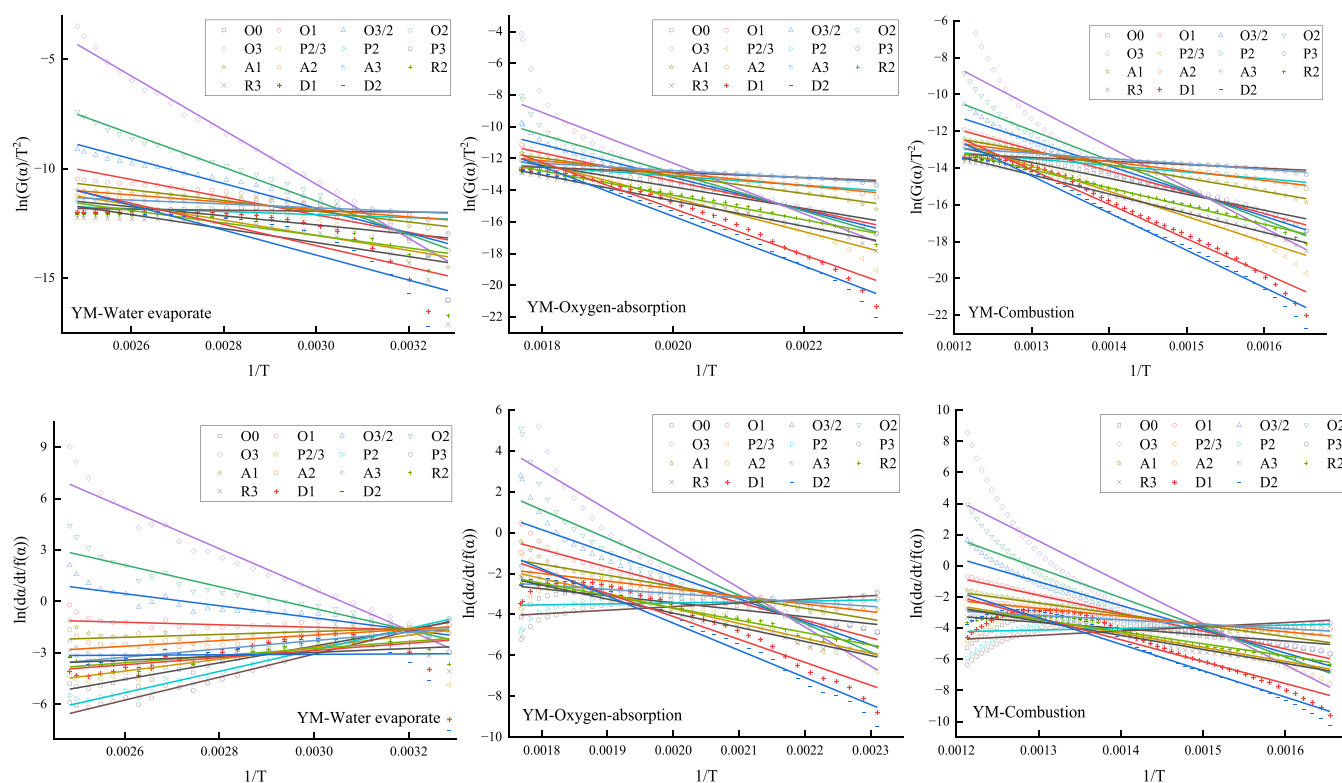
Figure 7. Calculation process of coal sample kinetics (with YM as an example).

Table 5. Results of Kinetic Parameter Calculations for Coal Samples

| samples	stage	mechanism function	Coats−Redfern method			Achar method		
			E(kJ/mol)	A	R^2	E(kJ/mol)	A	R^2
YM	water evaporation	O3	102.7	1.75×10^{16}	0.990	98.9	6.24×10^{15}	0.967
	oxygen absorption	O1	73.9	3.39×10^6	0.994	72.0	2.62×10^6	0.968
	combustion	O1	96.2	4.43×10^5	0.994	95.6	4.70×10^5	0.982
O70	water evaporation	O3	102.3	1.51×10^{16}	0.990	101.0	1.22×10^{16}	0.967
	oxygen absorption	O1	74.7	4.04×10^6	0.994	77.5	9.08×10^6	0.968
	combustion	O1	96.0	4.47×10^5	0.994	95.5	4.74×10^5	0.982
O110	water evaporation	O3	78.8	2.14×10^{12}	0.990	74.0	5.64×10^{11}	0.967
	oxygen absorption	O1	94.8	4.20×10^8	0.994	88.0	1.02×10^8	0.968
	combustion	O1	95.1	3.80×10^5	0.994	94.6	4.06×10^5	0.982
O180	water evaporation	O3	72.1	1.60×10^{11}	0.990	67.2	3.83×10^{10}	0.967
	oxygen absorption	O1	105.6	4.79×10^9	0.994	114.5	4.38×10^{10}	0.968
	combustion	O1	92.2	2.33×10^5	0.994	93.3	3.26×10^5	0.982

beginning and end of the reaction, respectively, and M is the coal sample mass during the reaction.

$$\alpha = \frac{M_0 - M}{\Delta M} = \frac{M_0 - M}{M_0 - M_e} \qquad (4)$$

In eqs 2 and 3, the key to calculating accurate kinetics parameters is to determine the accurate mechanism function, that is, the most probable mechanism function. If the kinetic parameters calculated by Achar and Coats−Redfern methods are close to the fit of the simultaneous curve, then this kinetic parameter can be considered to be the kinetic parameter of the real coal oxygen reaction. The mechanism function is also the most probable mechanism function. This method is also known as the Bagchi method. According to the Bagchi method, the 15 commonly used mechanism functions for coal oxygen reactions are shown in Table 4.[47,48]

The 15 commonly used mechanistic functions for gas−solid reactions in Table 4 were brought into eqs 2 and 3 for calculation and fitting, as shown in Figure 7. Significant differences can be observed in the kinetic parameters obtained by fitting different mechanistic functions for different stages. The kinetic parameters of the reactions at different stages of coal secondary spontaneous combustion obtained by the differential and integral methods are illustrated in Table 5. The results show that the water evaporation stage corresponds to an O3 reaction, while the oxygen adsorption and combustion stages are both O1 reactions for the spontaneous combustion of raw coal and the secondary spontaneous combustion of preoxidized coal. This notion indicates that preoxidation does not change the chemical nature of the reaction between coal and oxygen. The average of the two calculated activation energies was taken as the true value of the apparent activation energy for the different reaction stages, as shown in Figure 8.
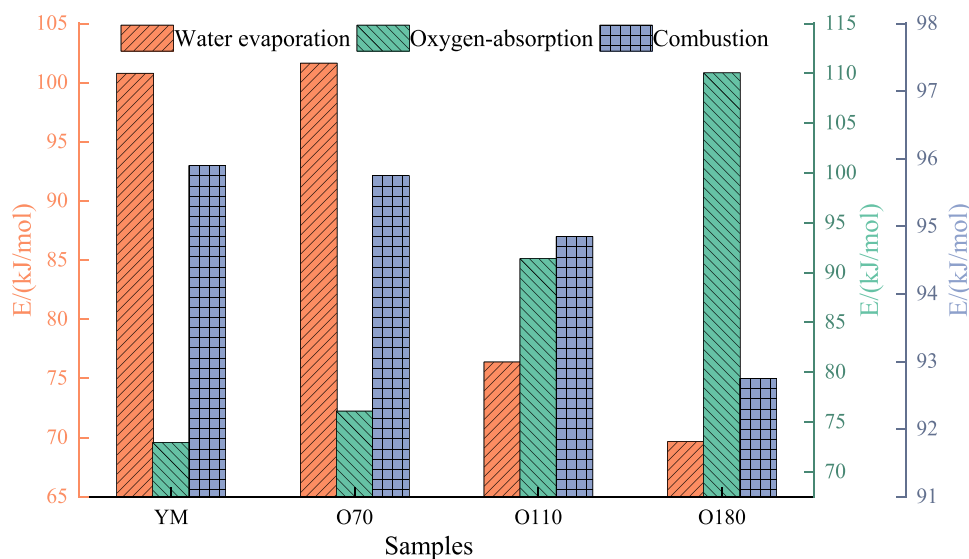
Figure 8. Comparison of the apparent activation energy of coal samples.

The effects of preoxidation on the different stages of spontaneous combustion are different. In the water evaporation stage, the apparent activation energy of the O70 coal was slightly higher than that of YM, while those of O110 and O180 were significantly lower than that of YM. This finding indicates that the water evaporation process of the O70 coal sample was slightly inhibited, while those of O110 and O180 were promoted. In the oxygen absorption stage, the apparent activation energy of the reaction gradually increased with the increase in the preoxidation temperature, indicating that preoxidation is not conducive to the adsorption of coal and oxygen. Furthermore, the apparent activation energy of preoxidized coal gradually decreased with the increase in the preoxidation temperature. However, the apparent activation energy of the combustion stage change is minor compared with the apparent activation energy of the other stages. For example, the average rate of change in apparent activation energy was 18.7% during the water evaporation stage, increasing to 26.8% during the oxygen absorption stage and only 1.5% during the combustion stage. This notion implies that the contribution of preoxidation to the combustion phase of coal is extremely low, which remains consistent with the results in Figure 6.

4. CONCLUSIONS AND OUTLOOKS

In this work, FTIR, laser thermal conductivity, and thermogravimetric experiments were used to investigate the key groups of preoxidized coal and the thermophysical properties and mass change characteristics of secondary spontaneous combustion with the following results. With the increase in the preoxidation temperature, the content of aromatic hydrocarbon compounds in coal gradually decreases, the aliphatic hydrocarbon compounds first increase and then decrease, and different oxygen-containing functional groups show different change trends. Preoxidation promotes the cracking of aromatic hydrocarbons and the oxidation of oxygen-containing functional groups in coal. The thermal diffusivity of coal gradually decreases after preoxidation, while the specific heat capacity and thermal conductivity first increase and then decrease. The process of spontaneous combustion of raw and preoxidized coals can be divided into

three stages: moisture evaporation, oxygen absorption, and combustion. The apparent activation energy of coal first increases and then decreases in the water evaporation stage, gradually increases in the oxygen absorption stage, and slowly decreases in the combustion stage with the increase in the preoxidation temperature. Preoxidation has a greater effect on the duration and apparent activation energy in the moisture evaporation and oxygen absorption stages and a smaller effect on the combustion stage. O70 has the shortest duration of the moisture evaporation stage and the longest oxygen absorption stage, while O180 shows the opposite trend.

In future research, we will continue to study the influence of the oxygen concentration, heating rate, and oxidation time on the secondary spontaneous combustion of coal in the preoxidation process.

■ AUTHOR INFORMATION

Corresponding Author

Tianjun Zhang − *College of Safety Science and Engineering, Xi'an University of Science and Technology, Xi'an 710054, China; Key Laboratory of Western Mine Exploitation and Hazard Prevention of the Ministry of Education, Xi'an 710054, China*; Email: 3537015423@qq.com

Authors

Jiangbo Guo − *College of Safety Science and Engineering, Xi'an University of Science and Technology, Xi'an 710054, China; Key Laboratory of Western Mine Exploitation and Hazard Prevention of the Ministry of Education, Xi'an 710054, China;* orcid.org/0000-0002-8252-6342
Hongyu Pan − *College of Safety Science and Engineering, Xi'an University of Science and Technology, Xi'an 710054, China; Key Laboratory of Western Mine Exploitation and Hazard Prevention of the Ministry of Education, Xi'an 710054, China*

Complete contact information is available at:
https://pubs.acs.org/10.1021/acsomega.2c07281

Notes

The authors declare no competing financial interest.

■ REFERENCES

(1) Qu, L.; Song, D.; Tan, B. Research on the critical temperature and stage characteristics for the spontaneous combustion of different metamorphic degrees of coal. *Int. J. Coal Prep. Util.* **2018**, *38*, 221−236.

(2) Zhang, Y.; Zhang, Y.; Li, Y.; Shi, X.; Zhang, Y. Heat effects and kinetics of coal spontaneous combustion at various oxygen contents. *Energy* **2021**, *234*, No. 121299.

(3) Zhang, L.; Wu, X.; Chiu, Y.; Pang, Q.; Shi, Z. Assessing integrated coal production and land reconstruction systems under extreme temperatures. *Expert Syst. Appl.* **2022**, *204*, No. 117560.

(4) BP p.l.c.*Statistical Review of World Energy 2022*, 2021.

(5) Zhang, Y.; Zhang, Y.; Li, Y.; Li, Q.; Zhang, J.; Yang, C. Study on the characteristics of coal spontaneous combustion during the development and decaying processes. *Process Saf. Environ. Prot.* **2020**, *138*, 9−17.

(6) Onifade, M.; Genc, B. Spontaneous combustion liability of coal and coal-shale: a review of prediction methods. *Int. J. Coal Sci. Technol.* **2019**, *6*, 151−168.

(7) Kuenzer, C.; Stracher, G. Geomorphology of coal seam fires. *Geomorphology* **2012**, *138*, 209−222.

(8) Cheng, J.; Wu, Y.; Dong, Z.; Zhang, R.; Wang, W.; Wei, G.; Chu, T.; Yu, Z.; Qin, Y.; Liu, G.; Li, H. A novel composite inorganic retarding gel for preventing coal spontaneous combustion. *Case Stud. Therm. Eng.* **2021**, *28*, No. 101648.

(9) Cheng, J.; Ma, Y.; Lu, W.; Liu, G.; Cai, F. Using inverting CO critical value to predict coal spontaneous combustion severity in mine gobs with considering air leakages-A case study. *Process Saf. Environ. Prot.* **2022**, *167*, 45−55.

(10) Lu, X.-x.; Wang, M.; Xue, X.; Xing, Y.; Shi, G.; Shen, C.; Yang, Y.; Li, Y. An novel experimental study on the thermorunaway behavior and kinetic characteristics of oxidation coal in a low temperature reoxidation process. *Fuel* **2022**, *310*, No. 122162.

(11) Zhou, F.-b.; Li, J.; He, S.; Liu, Y. Experimental modeling study on the reignition phenomenon when opening a sealed fire zone. *Procedia Earth Planet. Sci.* **2009**, *1*, 161−168.

(12) Xiao, Y.; Ren, S.; Deng, J.; Shu, C. Comparative analysis of thermokinetic behavior and gaseous products between first and second coal spontaneous combustion. *Fuel* **2018**, *227*, 325−333.

(13) Pan, R.; Wang, C.; Chao, J.; Jia, H.; Wang, J. Experimental research on the characteristics of the secondary oxidation heat of different unloaded coals. *Fuel* **2022**, *307*, No. 121939.

(14) Tang, Y.; Xue, S. Laboratory study on the spontaneous combustion propensity of lignite undergone heating treatment at low temperature in inert and low-oxygen environments. *Energy Fuels* **2015**, *29*, 4683−4689.

(15) Xiao, Y.; Ye, X.; Liu, K.; Chen, L. Transformation law of key functional groups in the process of coal secondary oxidation. *J. China Coal Soc.* **2022**, *46*, 989−1000.

(16) Liang, Y.; Tian, F.; Luo, H.; Tang, H. Characteristics of coal re-oxidation based on microstructural and spectral observation. *Int. J. Min. Sci. Technol.* **2015**, *25*, 749−754.

(17) Zhao, D.; Liu, H.; Zhu, D.; Qin, M. Effect of O-containing functional groups produced by preoxidation on Zhundong coal gasification. *Fuel Process. Technol.* **2020**, *206*, No. 106480.

(18) Jo, W.; Choi, H.; Kim, S.; Yoo, J.; Chun, D.; Rhim, Y.; Lin, J.; Lee, S. Changes in spontaneous combustion characteristics of low-rank coal through pre-oxidation at low temperatures. *Korean J. Chem. Eng.* **2015**, *32*, 255−260.

(19) Xu, Y.; Bu, Y.; Liu, Z.; Lv, Z.; Chen, M.; Wang, L. Effect of the reignition characteristics on long-flame coal by oxidization and water immersion. *Environ. Sci. Pollut. Res.* **2021**, *28*, 57348−57360.

(20) Xu, Q.; Yang, S.; Yang, W.; Tang, Z.; Hu, X.; Song, W.; Zhou, B. Z.; Yang, K. Secondary oxidation of crushed coal based on free radicals and active groups. *Fuel* **2021**, *290*, No. 120051.

(21) Álvarez, T.; Fuertes, A.; Pis, J.; Ehrburger, P. Influence of coal oxidation upon char gasification reactivity. *Fuel* **1995**, *74*, 729−735.

(22) Pis, J.; de La Puente, G.; Fuente, E.; Morán, A.; Rubiera, F. A study of the self-heating of fresh and oxidized coals by differential thermal analysis. *Thermochim. Acta* **1996**, *279*, 93−101.

(23) Wang, K.; Liu, X.; Deng, J.; Zhang, Y.; Jiang, S. Effects of pre-oxidation temperature on coal secondary spontaneous combustion. *J. Therm. Anal. Calorim.* **2019**, *138*, 1363−1370.

(24) Wang, K.; Fan, H.; Gao, P.; He, Y.; Shu, P. Spontaneous combustion characteristics of wetting coal under different prepyrolysis temperatures. *ACS Omega* **2020**, *5*, 33347−33356.

(25) Wang, K.; Gao, P.; Sun, W.; Fan, H.; He, Y.; Han, T. Thermal behavior of the low-temperature secondary oxidation of coal under different pre-oxidation temperatures. *Combust. Sci. Technol.* **2022**, *194*, 1712−1729.

(26) Tang, Y.; Wang, H. Experimental investigation on micro-structure evolution and spontaneous combustion properties of secondary oxidation of lignite. *Process Saf. Environ. Prot.* **2019**, *124*, 143−150.

(27) Deng, J.; Zhao, J.; Zhang, Y.; Huang, A.; Liu, X.; Zhai, X.; Wang, C. Thermal analysis of spontaneous combustion behavior of partially oxidized coal. *Process Saf. Environ. Prot.* **2016**, *104*, 218−224.

(28) Lü, H.-F.; Deng, J.; Li, D.; Xu, F.; Xiao, Y.; Shu, C. Effect of oxidation temperature and oxygen concentration on macro character-istics of pre-oxidised coal spontaneous combustion process. *Energy* **2021**, *227*, No. 120431.

(29) Zhang, Y.; Wu, B.; Liu, S.; Lei, B.; Zhao, J.; Zhao, Y. Thermal kinetics of nitrogen inhibiting spontaneous combustion of secondary oxidation coal and extinguishing effects. *Fuel* **2020**, *278*, No. 118223.

(30) Yan, H.; Nie, B.; Liu, P.; Chen, Z.; Yin, F.; Gong, J.; Lin, S.; Wang, X.; Kong, F.; Hou, Y. Experimental assessment of multi-parameter index gas correlation and prediction system for coal spontaneous combustion. *Combust. Flame* **2023**, *247*, No. 112485.

(31) Deng, J.; Bai, Z. J.; Xiao, Y.; Shu, C. M.; Laiwang, B. Effects of imidazole ionic liquid on macroparameters and microstructure of bituminous coal during low-temperature oxidation. *Fuel* **2019**, *246*, 160−168.

(32) Zheng, Y.; Li, Q.; Lin, B.; Zhou, Y.; Liu, Q.; Zhang, G.; Zhao, Y. Real-time analysis of the changing trends of functional groups and corresponding gas generated law during coal spontaneous combus-tion. *Fuel Process. Technol.* **2020**, *199*, No. 106237.

(33) Chen, C.; Tang, Y.; Guo, X. Comparison of structural characteristics of high-organic-sulfur and low-organic-sulfur coal of various ranks based on FTIR and Raman spectroscopy. *Fuel* **2022**, *310*, No. 122362.

(34) Gao, D.; Guo, L.; Wang, F.; Zhu, L.; Gao, Z. Investigation on thermal analysis and FTIR microscopic characteristics of artificially-oxidized coal and chronic naturally-oxidized coal during secondary oxidation. *Fuel* **2022**, *327*, No. 125151.

(35) Ma, L.; Yu, W.; Ren, L.; Qin, X.; Wang, Q. Micro-characteristics of low-temperature coal oxidation in CO_2/O_2 and N_2/O_2 atmospheres. *Fuel* **2019**, *246*, 259−267.

(36) Qi, X.; Wang, D.; Xin, H.; Qi, G. An in situ testing method for analyzing the changes of active groups in coal oxidation at low temperatures. *Spectrosc. Lett.* **2014**, *47*, 495−503.

(37) Zhang, Y.; Zhang, Y.; Shi, X.; Liu, S.; Shu, P.; Xia, S. Investigation of thermal behavior and hazards quantification in spontaneous combustion fires of coal and coal gangue. *Sci. Total Environ.* **2022**, *843*, No. 157072.

(38) Deng, J.; Ren, S.; Xiao, Y.; Li, Q.; Shu, C. Thermal properties of coals with different metamorphic levels in air atmosphere. *Appl. Therm. Eng.* **2018**, *143*, 542−549.

(39) Zhang, Y.; Zhang, Y.; Shi, X.; Li, Y.; Zhang, X. Co-spontaneous combustion of coal and gangue: Thermal behavior, kinetic character-istics and interaction mechanism. *Fuel* **2022**, *315*, No. 123275.

(40) Zhang, Y.; Zhang, Y.; Li, Y.; Shi, X.; Che, B. Determination of ignition temperature and kinetics and thermodynamics analysis of high-volatile coal based on differential derivative thermogravimetry. *Energy* **2022**, *240*, No. 122493.

(41) Xiao, H.-m.; Ma, X.; Lai, Z. Isoconversional kinetic analysis of co-combustion of sewage sludge with straw and coal. *Appl. Energy* **2009**, *86*, 1741−1745.

(42) Chen, P.; Zhang, L.; Huang, K. Kinetic modeling of coal thermal decomposition under air atmosphere. *Energy Fuels* **2016**, *30*, 5158−5166.

(43) Wang, Y.; Song, Y.; Zhi, K.; Li, Y.; Teng, Y.; He, R.; Liu, Q. Combustion kinetics of Chinese Shenhua raw coal and its pyrolysis carbocoal. *J. Energy Inst.* **2017**, *90*, 624−633.

(44) Deng, J.; Yang, Y.; Zhang, Y.; Liu, B.; Shu, C. Inhibiting effects of three commercial inhibitors in spontaneous coal combustion. *Energy* **2018**, *160*, 1174−1185.

(45) Liao, X.; Zhang, S.; Wang, X.; Shao, J.; Zhang, X.; Wang, X. H.; Yang, H. P.; Chen, H. Co-combustion of wheat straw and camphor wood with coal slime: Thermal behavior, kinetics, and gaseous pollutant emission characteristics. *Energy* **2021**, *234*, No. 121292.

(46) Rego, F.; Dias, A.; Casquilho, M.; Rosa, F.; Rodrigues, A. Pyrolysis kinetics of short rotation coppice poplar biomass. *Energy* **2020**, *207*, No. 118191.

(47) Dhyani, V.; Kumar, J.; Bhaskar, T. Thermal decomposition kinetics of sorghum straw via thermogravimetric analysis. *Bioresour. Technol.* **2017**, *245*, 1122−1129.

(48) Yuan, L.; Smith, A. CO and CO_2 emissions from spontaneous heating of coal under different ventilation rates. *Int. J. Coal Geol.* **2011**, *88*, 24−30.